

# FLUORESCENCE-ACTIVATED CELL SORTING AND ITS APPLICATIONS

MICHAEL H. JULIUS, RICHARD G. SWEET, C. GARRISON FATHMAN,\*  
and LEONARD A. HERZENBERG  
Department of Genetics, Stanford University School of Medicine,  
Stanford, California

---

## ABSTRACT

The Fluorescence Activated Cell Separator (FACS) separates cells according to fluorescence, light-scattering characteristics, or selected combinations of these two parameters. The instrument can process up to 5000 cells/sec and separate two nearly pure fractions with independently specified ranges of fluorescence and light-scattering cross sections for each fraction. The FACS can differentiate between viable and dead cells on the basis of light scattering. Appropriate threshold setting permits "gating out" of the dead-cell population so that cell populations can be separated or analyzed on the basis of viable-cell content. Using the FACS in combination with fluorescein-conjugated antigens to visualize antigen-binding cells by fluorescence, we have obtained viable and functional populations of antigen-binding cells enriched up to 400-fold from spleens of primed and unprimed mice. We have directly demonstrated that antigen-binding cells in both primed and unprimed mouse spleen contain the precursors of antibody-forming cells. Moreover, the antigen-binding precursor cells are functionally specific, and the avidity of the antibody formed is directly correlated with the avidity of the antigen receptors on the antigen-binding precursor cells.

## DESCRIPTION OF THE INSTRUMENT

The Fluorescence Activated Cell Separator (FACS) separates cells according to fluorescence, light-scattering characteristics, or selected combinations of the two parameters. Figure 1 is a simplified block diagram of the system. Cells in liquid suspension are forced under pressure through a micronozzle into the center of a stream of cell-free fluid and then out an effluent nozzle 50  $\mu\text{m}$  in diameter. This design creates a coaxial flow that keeps the cells near the axis of the effluent jet.

---

\*Present address: Immunology Branch, National Cancer Institute, National Institutes of Health, Bethesda, Md.

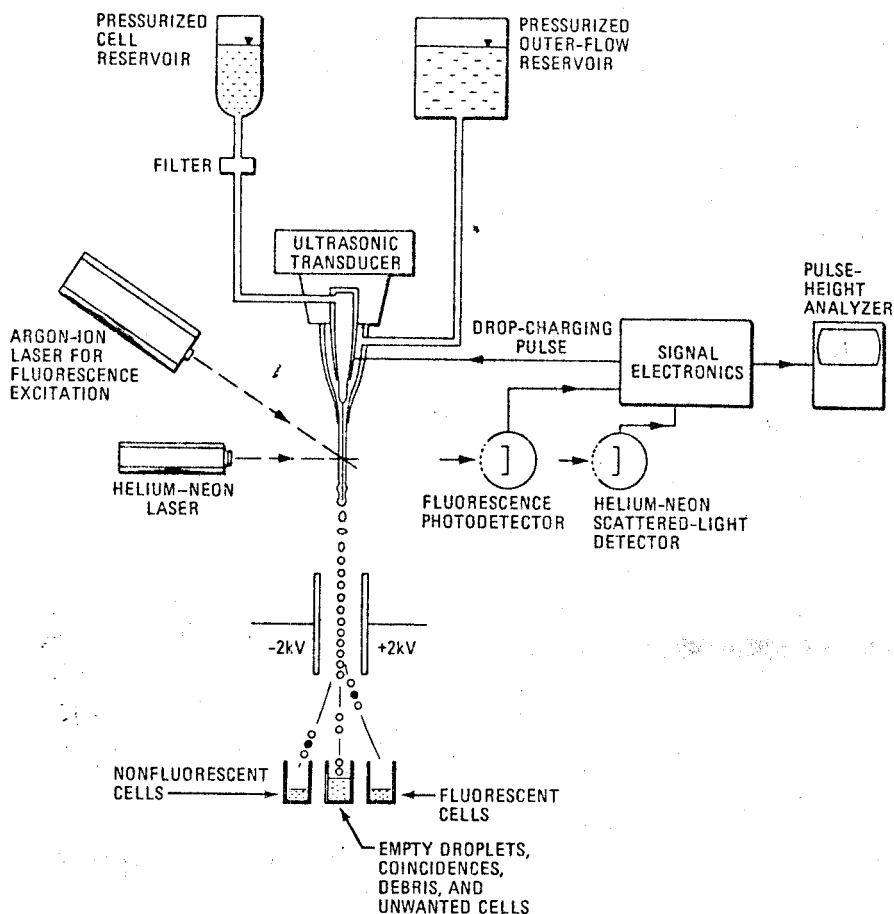


Fig 1 Simplified block diagram of the Fluorescence Activated Cell Separator (FACS).

The nozzle assembly is vibrated axially at 40 kHz, breaking the jet into 40,000 uniform droplets per second. Immediately below the nozzle, before droplet formation occurs, the jet is illuminated by two lasers. Low-angle scattered light from one, a helium-neon unit operating at 632.8 nm, falls on a red-sensitive photodetector and produces a signal related to cell volume. The second laser, an argon-ion unit operating at one of a number of lines between 454 and 514 nm, excites fluorescence in cells tagged with appropriate fluorescent material. Some of the fluorescent light falls on a second photodetector and provides a signal proportional to the number of fluorescent residues on the cell. Signals produced in the scatter and/or fluorescent channels are processed, delayed, and combined as required to produce electrical pulses, which are used to charge the liquid stream at the time the droplet containing the desired cell is forming. Droplets

broken off while the stream is charged retain their charge. Further downstream, the droplets pass through an electric field between two charged plates. Charged droplets are deflected appropriately, while uncharged droplets continue on their original course. The charging pulse lasts for three droplet periods, centered on the time the cell is expected to enter a droplet, to ensure that the droplet containing a desired cell is charged and thus deflected. The charging pulses are synchronized with the ultrasonic droplet generator so as to ensure that all drops formed during the charging period are equally charged. Further details of basic instrument operation can be found in the article by Bonner et al.<sup>1</sup> A more recent instrument, presently being tested, uses illumination by a single argon-ion laser for both scatter and fluorescence.

Analog signal pulses produced by the scatter and fluorescent-light detectors are converted to digital logic signals by circuits that respond only to signals within selected amplitude limits. These digital signals are combined logically to define two cell fractions, each fraction corresponding to scatter and fluorescence signal ranges that can be independently specified. Droplets containing cells in one fraction (D1) are deflected in one direction, and droplets containing cells in the other fraction (D2) are deflected in the opposite direction. Logic circuits prohibit deflection of droplets containing detected cells or particles not meeting the D1 or D2 criteria and cells too closely spaced to separate properly.

## INSTRUMENT PERFORMANCE

The instrument can detect fluorescence of single cells with more than 3000 bound molecules of fluorescein per cell. Cells or particles having a uniform fluorescence much greater than the detectable minimum produce a single amplitude distribution having a coefficient of variation of about 9%. This uncertainty in amplitude measurement, contributed by the instrument, defines its fluorescence amplitude resolving capability. The instrumental spread for scattered light signals from uniform spherical particles also corresponds to a coefficient of variation of about 9%, but signals from nonspherical cells may vary more than this because of differences in orientation as they cross the laser beam.

Final fraction purities of greater than 95% are typically obtained in a one-pass separation at processing rates up to 5000 cells/sec. At this processing rate, up to about 30% of the desired cells are too closely spaced for proper separation and are discarded in the nondeflected droplet fraction by the coincidence-detection circuits. For separation of cells comprising a relatively small fraction—less than about 3%—of the input sample, it is often faster to make a preliminary separation at a very high processing rate, e.g., 20,000 cells/sec or more. Since nearly every wanted cell is accompanied by one or more unwanted "passengers," the circuitry for discarding closely spaced cells must be disabled. The highly enriched separated fraction is then sorted again to achieve the desired final purity.

## ANALYTICAL APPLICATIONS OF THE FACS

The FACS has been used for analysis and cell separation. It has the useful capabilities of allowing analysis of murine lymphoid cells by two independent parameters—fluorescence and scatter. With appropriate fluorescein-conjugated antisera, it is possible to specifically label certain subpopulations for analysis or separation. This section describes two of the analytical applications of the FACS which were studied in this laboratory

### Detection of Dead Cells by Light Scattering

One application of the FACS which was recognized during early analytical studies is the detection and analysis of viable cells. Treatment of cell populations with the fluorogenic compound fluorescein diacetate (FDA) renders only viable cells fluorescent,<sup>2</sup> and the dead cells do not become fluorescent. Therefore, in a population treated with FDA, analysis of the scatter signals from fluorescent cells only (i.e., fluorescence-gated scatter, or FGS) generates the scatter profile of viable cells in that population. Figure 2 shows the scatter profile (S) of

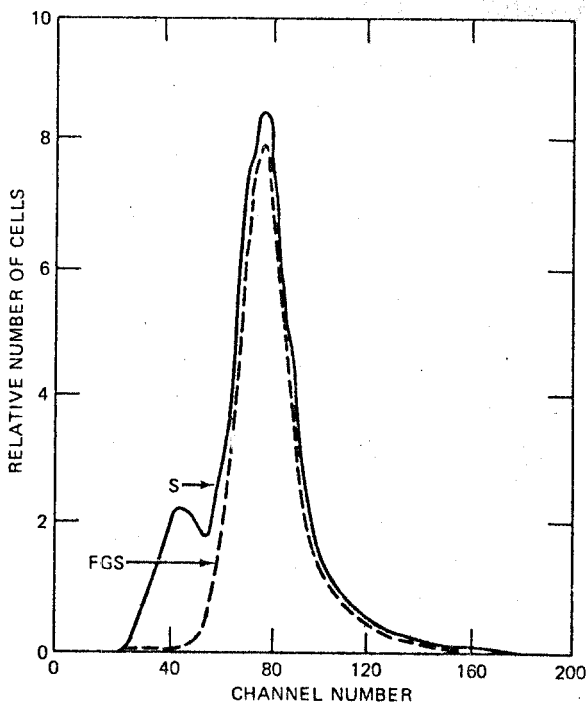


Fig 2 Scatter profile (S) of murine thymocytes compared with FGS profile of FDA-stained thymocytes.

murine thymocytes. Superimposed on this distribution is the FGS profile of FDA-fluorescent thymocytes. The nonfluorescent dead cells constitute a subpopulation that can be clearly differentiated on the basis of scatter alone. Appropriate threshold settings enable us to "gate out" the dead cells so that any subsequent separation or analysis of the population can be based on viable-cell content. This characteristic dead-cell scatter profile is obtained from cells of all lymphoid organs studied thus far.

### Detection of Functionally Distinct Cells by Immunofluorescent Staining and FGS

Murine lymphoid cells can be divided into two major subpopulations that contain cells with different functional characteristics and ontogeny. One subpopulation contains bone-marrow-derived B cells, which differentiate into antibody-forming cells.<sup>3</sup> The other major subpopulation contains cells that have undergone differentiation within the thymus and are required for the differentiation of B cells into antibody-forming cells in response to most antigens. These are called T cells.<sup>3</sup> The B cells bear easily detectable surface immunoglobulin,<sup>4</sup> whereas T cells bear the alloantigenic marker Thy-1 ( $\theta$ ).<sup>4</sup> With fluorescein-conjugated antibodies, it is possible to differentially label these cell types in single-cell suspensions of lymphoid organs. Once labeled, the cells can be analyzed by the FACS. Figure 3 shows the scatter profile (S) of splenic

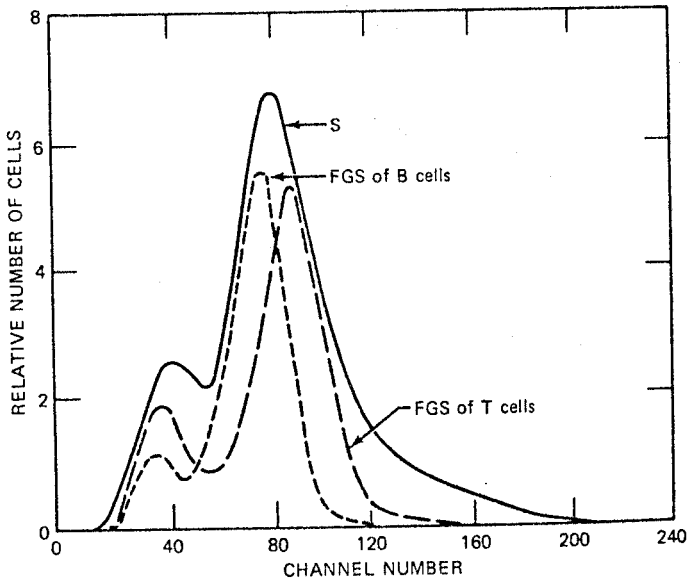


Fig. 3 Scatter profile (S) of splenic lymphocytes compared with FGS profiles of B and T cells.

lymphocytes with superimposed FGS profiles of T and B cells, detected by the appropriate fluorescent antisera.

It is apparent that T cells are larger than B cells. This is in agreement with the data of Howard, Hunt, and Gowans,<sup>5</sup> who used unit gravity sedimentation analysis of lymphocyte populations and assayed for the presence of T and B cells in the populations of cells sedimenting at various rates. They found that the more rapidly sedimenting (larger) cells were substantially enriched for T cells, whereas the majority of the more slowly sedimenting (smaller) cells were B cells. We also found that T and B cells present in lymph nodes exhibit the same scatter distribution as those in the spleen.

In addition to permitting us to routinely separate and analyze the viable cells in heterogeneous cell populations, the FACS provides a powerful tool in the analysis of functionally distinct cell subpopulations involved in the immune process.

### ISOLATION AND FUNCTIONAL CHARACTERIZATION OF ANTIBODY-FORMING CELL PRECURSORS IN MICE

The development of the FACS has enabled us to isolate functionally active populations of cells involved in the immune response. For the first time we have the opportunity to directly address two problems of long standing in cellular immunology.

First, are specific antigen-binding cells the precursors of antibody-forming cells? Other investigations have shown that depletion of specific antigen-binding cells from a lymphocyte population results in the inability of that population to respond to the specific antigen.<sup>6,7</sup> These studies, however, provide only indirect evidence for the precursor role of antigen-binding cells. We have isolated almost pure populations of antigen-binding cells from primed and unprimed mouse spleen and tested their ability to respond to antigen after being transferred into irradiated recipients. We have already established that a population of cells binding Keyhole Limpet Hemocyanin (KLH), isolated by the FACS from spleens of mice immunized with KLH, contains the precursors of anti-KLH antibody-forming cells necessary to give an adoptive secondary response.<sup>8</sup> Similarly, as the data presented here demonstrate, cells binding dinitrophenyl (DNP), isolated from unprimed mouse spleen, contain precursors of anti-DNP antibody-forming cells required for an adoptive primary response. Thus the precursors of antibody-forming cells in both primary and secondary adoptive responses are contained in the population of specific antigen-binding cells.

Second, since we can isolate precursors of specific antibody-forming cells, we can directly determine the relationship between the avidity of the antibody formed and the avidity of the antigen receptors on the isolated antigen-binding precursors. In adoptive-primary-transfer experiments, the avidity of anti-DNP antibody-forming cells in recipients of high-avidity DNP-binding cells was

100-fold higher than the avidity of the antibody-forming cells in recipients of unfractionated spleen. The data clearly demonstrate that high-avidity antigen-binding precursor cells give rise to high-avidity antibody-forming cells.

### **Demonstration That Antigen-Binding Cells Are Precursors of Antibody-Forming Cells**

#### *Adoptive Secondary Response to KLH: Functional Specificity of KLH-Binding Cells*

Having already established the precursor activity of KLH-binding cells derived from KLH-primed spleen,<sup>8</sup> we tested the functional specificity of these cells using the following experimental design. The KLH-binding cells were isolated (the FACS and fluorescein-conjugated KLH being used to visualize KLH-binding cells) from spleens doubly primed to KLH and Human Gamma Globulins (HGG), and the resulting population, depleted of KLH-binding cells, was tested (in separate groups of mice) for its ability to respond to KLH and HGG in an adoptive transfer. If the KLH-binding cells include only specific precursors for anti-KLH antibody-forming cells, then transfer of the depleted population should give a diminished anti-KLH response but an equivalent anti-HGG response in comparison to the responses of unfractionated spleen.

As the data in Table 1 show, transfer of unseparated KLH and HGG doubly primed spleen cells (containing 1% KLH-binding cells) into irradiated recipients gave an anti-KLH hemagglutination titer ( $\log_2$ ) of 8.4 and an anti-HGG titer ( $\log_2$ ) of 8.6 when challenged with KLH or HGG, respectively. No detectable anti-HGG titer resulted when KLH was used as the challenging antigen, and, conversely, no measurable anti-KLH titer resulted when HGG was used as the challenging antigen. When the population depleted (undeflected) of KLH-binding cells (containing <0.1% KLH-binding cells) was transferred and challenged with KLH, the resulting anti-KLH titer of 4.0 was more than tenfold lower than the titer elicited by transfer of unseparated spleen; however, when the undeflected population was challenged with HGG, the resulting anti-HGG titer of 9.6 was comparable to that given by unseparated spleen. Transfer of the population enriched for KLH-binding cells (70%) alone gave very little if any response to either KLH or HGG, but admixture with undeflected cells (Table 1) or a known source of cooperating cells<sup>8</sup> (which themselves do not respond) to the KLH-binding cells completely restored the anti-KLH response to the level of the unseparated spleen.

The depleted population from which the KLH-binding cells were isolated was unable to give an adoptive response to KLH, although it was as efficient as unseparated spleen cells in transferring a secondary response to an unrelated antigen, HGG. Thus the precursors of antibody-forming cells in a secondary response are detected only among antigen-binding cells, and these cells reflect the specificity of their commitment.

TABLE 1

FUNCTIONAL SPECIFICITY OF KLH-BINDING CELLS  
(Fluorescent Cells: Unseparated, 1%; Deflected, 70%; Undeflected, <0.1)

Number of cells transferred ( $\times 10^6$ )*			Antigen	Log <sub>2</sub> anti-KLH titer†	Log <sub>2</sub> anti-HGG titer†
Unsep.	Defl.	Undefl.			
3			KLH	8.4 ± 0.8	<1
		3	KLH	4.0 ± 0.5	<1
		0.05	KLH	1.4 ± 0.4	<1
		0.05	3	KLH	8.2 ± 0.4
3			HGG	<1	8.6 ± 0.2
		3	HGG	<1	9.6 ± 0.5
		0.05	HGG	<1	<1
		0.05	3	HGG	<1

\*Spleen cells from KLH and HGG doubly primed mice were transferred into irradiated (600 R) congenic hosts along with  $3 \times 10^6$  congenic bone-marrow cells and either 100  $\mu$ g KLH or 400 mg heat-aggregated HGG.

†Log<sub>2</sub> titers (0.01M dithioerythritol resistant) ± standard error at day 15 after transfer. Four animals per group.

### Adoptive Primary Response to DNP

Adoptive primary responses are inefficient with respect to the number of cells required to transfer a response compared to the number for adoptive secondary responses. This relative inefficiency is due to the limiting number of cooperators available in unprimed spleen populations. To study the adoptive primary response to DNP, we are using the DNP-KLH hapten-carrier system since carrier primed cooperators greatly increase the efficiency of the response. Since we are interested in finding out whether isolated DNP-binding cells contain the precursors for anti-DNP antibody-forming cells, populations of carrier primed cooperators (required for the differentiation and maturation of DNP-precursor cells) must be depleted of DNP-precursor cells that would be confused with the activity of the isolated DNP-binding cells. To remove precursors from the cooperator population, we used the nylon wool depletion method developed originally for this purpose in this laboratory.<sup>9</sup>

As shown in Table 2, KLH-primed spleen, containing 44% immunoglobulin-bearing (B) cells and 46% thymus-derived (T) cells as assayed by immunofluorescence, after being transferred into irradiated recipients resulted in  $21 \times 10^3$  antibody-forming cells (plaque-forming cells, or PFC) per spleen (measured in the Cunningham plaquing assay)<sup>10</sup> and an anti-KLH hemagglutination titer of 1100. Incubation of KLH-primed spleen with nylon wool resulted in a tenfold depletion of immunoglobulin-bearing cells (4%) and a complementary twofold enrichment of T cells (89%). The T-cell-enriched



population was depleted of both the ability to transfer a primary response to DNP, giving rise to  $2 \times 10^3$  PFC per spleen, and the ability to transfer a secondary response to KLH, resulting in an anti-KLH titer of 17. Thus the nylon wool efficiently removes DNP-precursor cells as well as KLH-memory B cells. However, the T-cell-enriched population contained the same cooperator activity per T cell as did the intact (unfiltered) KLH-primed spleen. Transfer of KLH-primed T cells with unprimed spleen, providing a source of DNP-precursor cells, resulted in  $49 \times 10^3$  PFC per spleen (Table 2). The anti-DNP response was twice that obtained with unfiltered KLH-primed spleen since T cells are limiting and the number of T cells transferred was double the number present in unfiltered primed spleen.

#### *Isolation and the Adoptive Response of DNP-Binding Cells*

The DNP-binding cells present in unprimed spleen populations were visualized by staining spleen cell suspensions with fluorescein-conjugated DNP mouse immunoglobulin ( $F^DNP$ -MIg). As shown in Table 3, the proportion of detectable DNP-binding cells depends on the concentration of  $F^DNP$ -MIg used in the staining procedure. If unprimed spleen is stained with  $F^DNP$ -MIg at 55  $\mu\text{g/ml}$ , 0.77% of the population binds detectable quantities. However, if a

TABLE 2

#### REMOVAL OF B PRECURSOR AND MEMORY CELLS BY NYLON WOOL

Cells transferred*	Percent† stained		Direct anti-DNP PFC per spleen‡ ( $\times 10^2$ )	Anti-KLH titer§
	Ig	T		
KLH-primed spleen¶	44%	46%	210	1100
KLH-primed T cells** (nylon wool column effluent)	4%	89%	20	17
Unprimed spleen	Not done		16	20
KLH-primed T cells plus unprimed spleen	Not done		490	140

\*Irradiated (600 R) animals received  $5 \times 10^6$  of each cell type and 100  $\mu\text{g}$  alum-precipitated DNP-KLH on day 0. Animals were boosted with 10  $\mu\text{g}$  DNP-KLH (aqueous) on day 5 and were bled and sacrificed on day 12.

†Indirect stain with either rabbit anti-MIg or anti-T and  $R_g$  goat anti-RIg (rhodamine-conjugated goat anti-rabbit Ig).

‡Arithmetic mean.

§Geometric mean.

¶Primed with 100  $\mu\text{g}$  KLH (aqueous) 3 months before sacrifice.

\*\*KLH-primed spleen depleted of Ig-bearing cells by passage through nylon wool column.

TABLE 3  
INHIBITION OF DNP-BINDING CELLS

Staining concentration of FDNP-MIg, $\mu\text{g/ml}$	Molarity of DNP on $^{\text{F}}$ DNP-MIg	Molarity of $\epsilon$ -DNP-lysine in staining mixture	Percent labeled cells	Percent inhibition
55	$8.7 \times 10^{-6}$	*	0.77*	
		$8.7 \times 10^{-5}$	0.63	18
		$8.7 \times 10^{-4}$	0.64	18
18	$2.9 \times 10^{-6}$		0.22†	
		$2.9 \times 10^{-5}$	0.12	45
		$2.9 \times 10^{-4}$	0.05	77
6	$9.7 \times 10^{-2}$		0.04‡	
		$9.7 \times 10^{-6}$	0.02	55
		$9.7 \times 10^{-5}$	0.009	78

\*3000 lymphocytes counted.

†10,000 lymphocytes counted.

‡30,000 lymphocytes counted.

concentration of 6  $\mu\text{g/ml}$  is used in the staining procedure, only 0.04% of the spleen cells bind detectable quantities of  $^{\text{F}}$ DNP-MIg. Moreover, if we try to inhibit the binding of  $^{\text{F}}$ DNP-MIg by staining in the presence of excess quantities of  $\epsilon$ -DNP-lysine, which will compete with the  $^{\text{F}}$ DNP-MIg for available binding sites on the cell surface, only the DNP-binding cells visualized by using low concentrations of  $^{\text{F}}$ DNP-MIg are easily inhibitable (Table 3). Presumably only high-avidity binding cells are labeled at low antigen concentration and are readily inhibitable with excess antigen, whereas higher concentrations of antigen are required to visualize lower avidity binding cells which are less readily inhibited by excess antigen.

Table 4 illustrates the adoptive primary response of isolated DNP-binding cells. In this experiment a high concentration of  $^{\text{F}}$ DNP-MIg (150  $\mu\text{g/ml}$ ) was used to visualize the DNP-binding cells in unprimed spleen. In the unseparated spleen population, 1.5% of the cells bound detectable antigen and were isolated by the FACS. The purified (deflected) population contained 90% DNP-binding cells, while the depleted (undeflected) population contained 0.2% DNP-binding cells. In the transfer of unseparated spleen cells, KLH-primed (T) cooperators, the deflected population, or the undeflected population alone, low but detectable anti-DNP PFC responses were obtained. When  $5 \times 10^6$  unseparated cells were combined with  $7.5 \times 10^6$  cooperators and transferred, the resulting response was  $28 \times 10^3$  anti-DNP PFC per spleen. Transfer of only  $5 \times 10^4$  purified DNP-binding cells with  $7.5 \times 10^6$  cooperators gave a comparable response,  $23 \times 10^3$  anti-DNP PFC per spleen. Thus, by enriching for

DNP-binding cells in the deflected fraction, we have also enriched 100-fold for DNP-precursor activity.

Transfer of  $5 \times 10^6$  undeflected cells with  $7.5 \times 10^6$  cooperators resulted, as expected, in a diminished response,  $8 \times 10^3$  anti-DNP PFC per spleen, compared with unseparated spleen. Whether these PFC are qualitatively different from those derived on transfer of unseparated spleen is discussed further in the following section.

TABLE 4

ADOPTIVE RESPONSE OF DNP-BINDING CELLS  
(Fluorescent Cells: Unseparated, 1.5%; Deflected, 90%; Undeflected, 0.2%)

Unsep.	Number of cells transferred* ( $\times 10^6$ )			Direct anti-DNP PFC per spleen† ( $\times 10^3$ )
	KLH-primed T	Defl.	Undefl.	
5				4 (3 to 6)
	7.5			4 (2 to 7)
		0.05		0.2 (0.1 to 3)
5			5	0.6 (0.5 to 0.7)
	7.5			28 (25 to 32)
	7.5	0.05		23 (19 to 26)
	7.5		5	8 (8 to 9)

\*Cells were transferred into irradiated (600 R) congenic hosts intravenously. Animals received 100  $\mu$ g alum-precipitated DNP-KLH on day 0 and 10  $\mu$ g aqueous DNP-KLH on day 5 and were sacrificed on day 12.

†Geometric mean and standard error. Four animals per group.

### Relationship Between Avidity of DNP-Binding Precursor Cells and Avidity of Resulting Anti-DNP PFC

Analogous to the inhibition of DNP-binding cells with  $\epsilon$ -DNP-lysine, the avidity of PFC was determined by varying concentrations of  $\epsilon$ -DNP-lysine incorporated in the plaquing medium. High-avidity PFC will be inhibited by low concentrations of  $\epsilon$ -DNP-lysine, but inhibition of lower avidity PFC will require higher concentrations of  $\epsilon$ -DNP-lysine. Figure 4 shows the inhibition profiles of the adoptive primary response to DNP discussed in Table 4.

The inhibition curves for the unseparated whole spleen and for the purified DNP-binding cells are virtually identical and represent a heterogeneous population of PFC with respect to avidities. However, the depleted population (non-DNP-binding cells) which gave a reduced number of anti-DNP PFC (Table 4) exhibits a striking difference when the avidities of the PFC are compared with the other populations. The avidities of the PFC derived from the depleted population are at least 1000-fold lower than the avidities derived from

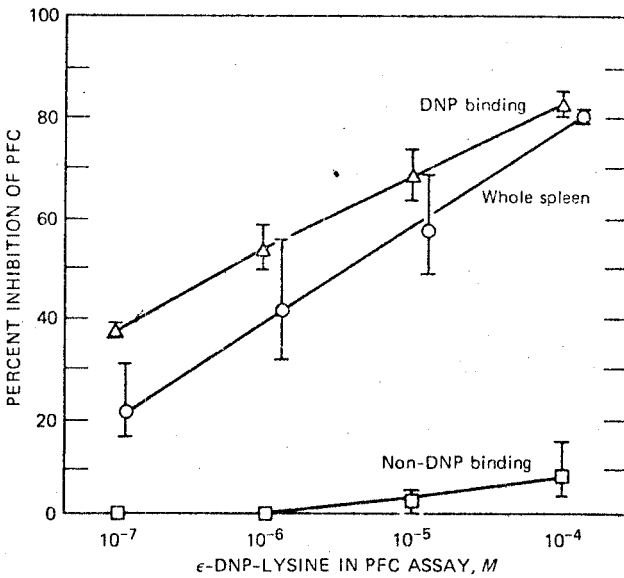


Fig. 4 Inhibition of anti-DNP PFC with  $\epsilon$ -DNP-lysine.

either the unseparated or the DNP-binding populations. Thus a concentration of  $^F$ DNP-MIg as high as 150  $\mu$ g/ml used to visualize DNP-binding cells is not sufficient to label all the DNP precursors since there appear to be DNP-precursor cells of sufficiently low binding avidity to be undetectable and therefore not separated.

These data led us to expect that, as we select higher avidity precursors, by decreasing the concentration of  $^F$ DNP-MIg used in staining, the avidity of the PFC derived from these precursors will increase. As a test of this prediction, DNP-binding cells visualized by using  $^F$ DNP-MIg at 10  $\mu$ g/ml were separated by the FACS. The results of the adoptive primary DNP transfer using these putatively high-avidity precursor cells are shown in Table 5.

Of the unseparated population, 0.2% bound detectable  $^F$ DNP-MIg. The deflected population contained 80% DNP-binding cells, and the undeflected fraction contained 0.01% binding cells. Transfer of  $5 \times 10^6$  unseparated cells with  $7.5 \times 10^6$  carrier primed cooperators again gave a much higher anti-DNP PFC response ( $77 \times 10^3$  PFC per spleen) than did  $5 \times 10^6$  unseparated cells transferred alone ( $21 \times 10^3$  PFC per spleen). Again transfer of primed cooperators, deflected population, or undeflected population alone gave low but detectable responses. The transfer of  $5 \times 10^4$  purified DNP-binding cells combined with  $7.5 \times 10^6$  carrier primed cooperators resulted in a significant response ( $27 \times 10^3$  PFC per spleen), indicating substantial enrichment of DNP-precursor activity concomitant with enrichment of DNP-binding cells.

Transfer of  $5 \times 10^6$  undeflected cells with  $7.5 \times 10^6$  primed cooperators resulted in  $22 \times 10^3$  PFC per spleen. The depleted response derived from the undeflected fraction was somewhat lower than what we would have predicted on the basis of the small fraction of DNP-binding cells removed.

Figure 5 represents the avidity profiles of the anti-DNP PFC responses derived from the different populations described in Table 5. The undeflected fraction shows the identical inhibition profile as the unseparated population. One might predict that if we had removed the high-avidity precursors from the undeflected fraction the resulting PFC should show a complementary depletion of high-avidity PFC. However, because the high-avidity PFC represent only a small proportion of the total response, we were unable to detect the depletion.

TABLE 5

ADOPTIVE RESPONSE OF HIGH-AVIDITY DNP-BINDING CELLS  
(Fluorescent Cells: Unseparated, 0.2%; Deflected, 80%; Undeflected, 0.01%)

Unsep.	Number of cells transferred* ( $\times 10^6$ )			Direct anti-DNP PFC per spleen† ( $\times 10^3$ )
	KLH-primed T	Defl.	Undefl.	
5	7.5	0.05	5	21 (17 to 27)
				4 (3 to 5)
				0.4 (0.3 to 0.5)
5	7.5	0.05	5	2 (1 to 3)
				77 (64 to 94)
	7.5			27 (17 to 43)
	7.5		5	22 (18 to 26)

\*Cells were transferred into irradiated (600 R) congenic hosts intravenously. Animals received 100  $\mu$ g alum-precipitated DNP-KLH on day 0 and 10  $\mu$ g aqueous DNP-KLH on day 5 and were sacrificed on day 12.

†Geometric mean and standard error. Four animals per group.

The inhibition profile of the anti-DNP PFC response derived from the purified DNP-binding cells is significantly different from the profiles of the other two populations. Purified DNP-binding cells gave rise to anti-DNP PFC that were 100-fold more avid than the PFC derived from either the unseparated or the undeflected populations. Thus high-avidity DNP-binding cells detected with low concentrations of  $^F$ DNP-MIg contain DNP precursors for high-avidity anti-DNP PFC.

Using the FACS, we have clearly demonstrated that antigen-binding cells in both primed and unprimed mouse spleen contain the precursors of antibody-forming cells. Moreover, the antigen-binding precursor cells are functionally specific, and the avidity of the antibody formed is directly correlated with the avidity of the antigen receptors on the antigen-binding precursors.

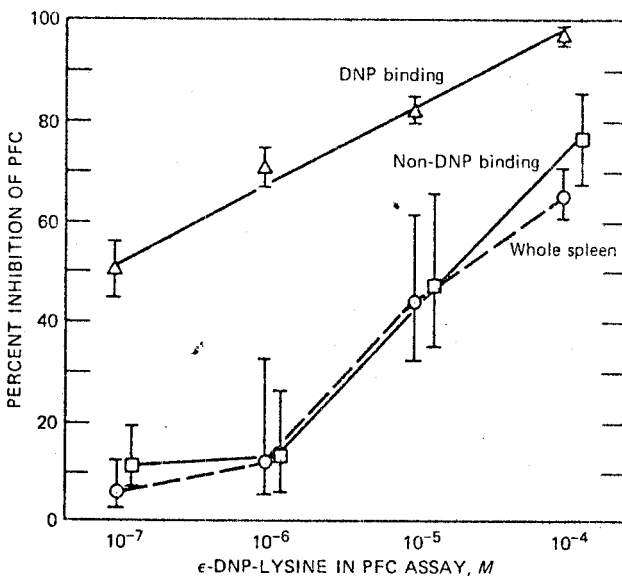


Fig. 5 Inhibition of anti-DNP PFC with  $\epsilon$ -DNP-lysine.

## ACKNOWLEDGMENTS

The work described in this paper was supported by National Institutes of Health grants AM-01-006 and GM 17367.

## REFERENCES

1. W. A. Bonner, H. R. Hulett, R. G. Sweet, and L. A. Herzenberg, Fluorescence Activated Cell Sorting, *Rev. Sci. Instrum.*, **43**: 404-409 (1972).
2. B. Rotman and B. W. Papermaster, Membrane Properties of Living Mammalian Cells as Studied by Enzymatic Hydrolysis of Fluorogenic Esters, *Proc. Nat. Acad. Sci. U.S.A.*, **55**: 134-141 (1966).
3. J. F. A. P. Miller and G. F. Mitchell, Thymus and Antigen Reactive Cells, *Transplant. Rev.*, **1**: 3-42 (1969).
4. M. C. Raff, Two Distinct Populations of Peripheral Lymphocytes in Mice Distinguishable by Immunofluorescence, *Immunology*, **19**: 637-650 (1970).
5. J. C. Howard, S. V. Hunt, and J. L. Gowans, Identification of Marrow-Derived and Thymus-Derived Small Lymphocytes in the Lymphoid Tissue and the Thoracic Duct Lymph of Normal Rats, *J. Exp. Med.*, **135**: 200-219 (1972).
6. G. L. Ada and P. Byrt, Specific Inactivation of Antigen-Reactive Cells with <sup>125</sup>I-Labelled Antigen, *Nature*, **222**: 1291-1292 (1969).
7. H. Wigzell and O. Makela, Separation of Normal and Immune Lymphoid Cells by Antigen-Coated Columns, *J. Exp. Med.*, **132**: 110-126 (1970).

8. M. H. Julius, T. Masuda, and L. A. Herzenberg, Demonstration That Antigen-Binding Cells Are Precursors of Antibody Producing Cells After Purification with a Fluorescence-Activated Cell Sorter, *Proc. Nat. Acad. Sci. U.S.A.*, **69**: 1934-1938 (1972).
9. M. H. Julius, E. Simpson, and L. A. Herzenberg, A Rapid Method for the Isolation of Functional Thymus-Derived Murine Lymphocytes, *Eur. J. Immunol.*, **3**: 645 (1973).
10. A. J. Cunningham and A. Szenberg, Further Improvements in the Plaque Technique for Detecting Single Antibody-Forming Cells, *Immunology*, **14**: 599-600 (1968).

